JOURNAL OF PHYSICAL ORGANIC CHEMISTRY
J. Phys. Org. Chem. 2000; **13:** 837–849

Multiphoton-absorbing organic materials for microfabrication, emerging optical applications and non-destructive three-dimensional imaging

Kevin D. Belfield,* Katherine J. Schafer, Yong Liu, Jun Liu, Xiaobin Ren and Eric W. Van Stryland

Department of Chemistry and School of Optics, University of Central Florida, P.O. Box 162366, Orlando, Florida 32816-2366, USA

Received 18 May 2000; revised 26 July 2000; accepted 27 July 2000

ABSTRACT: Non-resonant two-photon absorption (TPA) can be defined as the simultaneous absorption of two photons, via a virtual state, in a medium. TPA exhibits a quadratic dependence of absorption on the incident light intensity, resulting in highly localized photoexcitation. Recent developments in the design and synthesis of efficient, stable TPA organic materials are discussed. Microfabrication via two-photon induced free radical polymerization of acrylate monomers and cationic polymerization of epoxide monomers was accomplished using commercially available photoinitiators, and also a custom-made compound possessing high two-photon absorptivity. Two-photon facilitated photoisomerization of a fulgide in solution and in a polymer thin film demonstrated two-photon induced photochromism and its application in interferometric image recording, respectively. Greatly enhanced signal-to-noise ratios and resolution were achieved in the non-destructive three-dimensional two-photon fluorescence imaging of a polymer-coated substrate versus conventional single-photon laser scanning confocal microscopic imaging. Multifunctional TPA organic materials and fabrication of functional microstructures are also discussed. Copyright © 2000 John Wiley & Sons, Ltd.

KEYWORDS: two-photon absorption; microfabrication; photoisomerization; photo-polymerization; fluorescence imaging

INTRODUCTION

Organic materials exhibiting significant non-linear responses to applied electric or electromagnetic fields have attracted intense interest during the last few decades. Currently, organic materials occupy a prominent role in 2-D (linear) display technology based on specifically induced phase transitions in liquid crystalline materials, thereby altering their optical properties, and in the rapidly developing arena of organic light-emitting diodes (electroluminescent materials). Organic chromophores are becoming an integral component in second and third harmonic generation, devices for radiation frequency conversion and waveguides. Suitable materials for such applications manifest a non-linear optical response in the presence of an applied electric field, resulting in amplification of the particular optical property (e.g. refractive index change) relative to that obtained via a linear dependence. The end of the 20th century and the beginning of the 21st century have been accompanied by an ever pressing need for materials that exhibit amplification or respond in a highly non-linear manner to a particular stimulus. In particular, compounds that undergo strong non-linear, multiphoton absorption are being investigated as materials for a wide variety of potential applications in areas ranging from optical information storage, 3-D optical memories, biophotonics, materials science and photochemistry. For example, it is projected that a multiphoton-based 3-D optical volumetric memory will provide up to three orders of magnitude more information in the same size enclosure relative to a 2-D optical disk memory.[1]

The non-linear, multiphoton process of two-photon absorption (TPA) has been gaining greater interest among a number of multidisciplinary areas, particularly in the rapidly developing fields of multiphoton fluorescence imaging, optical data storage and switching, optical sensor protection, telecommunications, laser dyes, 3-D microfabrication and photodynamic therapy (PDT).[2–5] The demands of such applications exceed properties and reliabilities delivered by current organic materials, underscoring the need for increasingly sophisticated non-linear optical organic materials. Since the probability of a TPA process is proportional to the square of the

**Correspondence to:* K. D. Belfield, Department of Chemistry and School of Optics, University of Central Florida, P.O. Box 162366, Orlando, Florida 32816-2366, USA.
E-mail: kbelfiel@mail.ucf.edu
Contract/grant sponsor: National Science Foundation; *Contract/grant number:* ECS-9970078, DMR 9975773.
Contract/grant sponsor: Air Force Office of Scientific Research; *Contract/grant number:* F49620-93-C-0063.

incident light intensity, photoexcitation is spatially confined to the focal volume.[1] Such precise control of photoexcitation is intriguing, facilitating the development of new technologies, processes and materials that require 3-D spatial resolution of physical properties, both static (permanent) and dynamic (reversible).

The theory of the simultaneous absorption of two photons was developed by Goeppert-Mayer in 1931,[6] but remained mainly an intellectual curiosity until the advent of the pulsed laser providing very high-intensity light. For simplicity, two-photon absorption can be conceptualized from a semiclassical perspective.[1] In the TPA process, molecules exposed to high intensity light can undergo near simultaneous absorption of two photons mediated by a so-called 'virtual state,' a state with no classical analog. The combined energy of the two photons accesses a stable excited state of the molecule. If the two photons are of the same energy (wavelength), the process is referred to as degenerate TPA. On the other hand, if the two photons are of different energy (wavelength), the process is non-degenerate TPA.

As light passes through a molecule, the virtual state may form, persisting for a very short duration (of the order of a few femtoseconds). TPA can result if a second photon arrives before decay of this virtual state, with the probability of TPA scaling with the square of the light intensity. This process is generally termed simultaneous two-photon absorption. Two-photon absorption thus involves the *concerted* interaction of both photons that combine their energies to produce an electronic excitation analogous to that conventionally caused by a single photon of a correspondingly shorter wavelength. Unlike single-photon absorption, whose probability is linearly proportional to the incident intensity, the TPA process depends on both a spatial and temporal overlap of the incident photons and takes on a quadratic (non-linear) dependence on the incident intensity.

Two-photon transitions can be described by two different mechanistic types. For non-polar molecules with a low-lying, strongly absorbing state near the virtual level, only excited states that are forbidden by single-photon selection dipole rules can be populated via two-photon absorption (Type 1 in Fig. 1).[1] The probability that this low-lying state can contribute to the virtual state is predicted by Heisenberg's uncertainty principle, with a virtual state lifetime approximated as $h/(4\pi\Delta E)$, where h is Planck's constant and ΔE is the energy difference between the virtual and actual states. Using this equation, it is predicted that an allowed state can contribute to formation of the virtual state for time $t_{virtual}$ which is equal to about $h/(4\pi\Delta E)$ with the transition probability proportional to $\Delta\mu^2$. For example, a lifetime of ca 0.3 fs is estimated for a state separation of 0.1 eV. Two-photon absorptivity, δ, is expressed in Goeppert-Mayer units (GM), with 1 GM = 1×10^{-50} cm^4 s molecule^{-1} photon^{-1}. Molecules which undergo strong TPA via the Type 1 process have two-photon absorptivities up to 10 GM.[7]

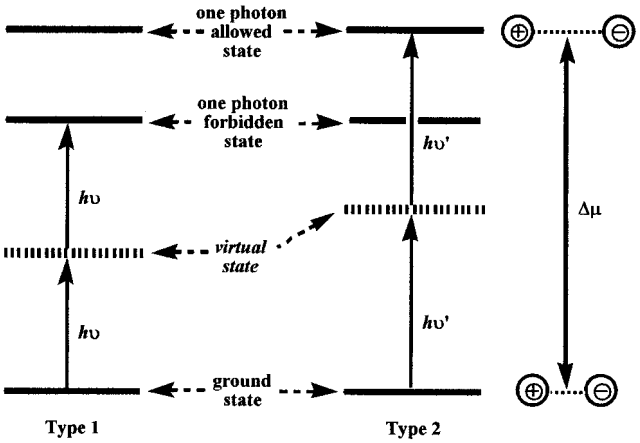

Figure 1. 'Simultaneous' two-photon absorption processes (Type 1 and 2)

In contrast, strong TPA can occur in polar molecules by a different mechanism (Type 2 in Fig. 1) in which a large change in dipole moment ($\Delta\mu > 10$ D) occurs upon excitation of the ground to an excited state.[1] Single-photon allowed states can then be accessed via TPA, and the virtual state lifetime is proportional to $\Delta\mu^2$, while the transition probability scales with $\Delta\mu^4$. In this case, both the ground and excited states can participate in the formation of the virtual state, enhancing TPA. In polar molecules with large $\Delta\mu$ between the ground and excited states, δ values in excess of 100 GM have been reported.[1,8]

The two-photon advantage

The quadratic, or non-linear, dependence of two-photon absorption on the intensity of the incident light has substantial implications. For example, in a medium containing one-photon absorbing chromophores, significant absorption occurs all along the path of a focused beam of suitable wavelength light. This can lead to out-of focus excitation. In a two-photon process, negligible absorption occurs except in the immediate vicinity of the focal volume of a light beam of appropriate energy. This allows spatial resolution about the beam axis as well as radially, which circumvents out-of-focus absorption and is the principle reason for two-photon fluorescence imaging.[9] Particular molecules can undergo upconverted fluorescence through non-resonant two-photon absorption using near-IR radiation, resulting in an energy emission greater than that of the individual photons involved (up-conversion). The use of a longer wavelength excitation source for fluorescence emission affords advantages not feasible using conventional UV or visible fluorescence techniques, e.g. deeper penetration of the excitation beam and reduction of photobleaching.

Argon ion (488 nm) and frequency-doubled Nd:YAG (532 nm) lasers are the commonly used light sources for

conventional (single-photon) laser scanning confocal microscopy (owing to their ready availability and low cost). Such light sources require fluorophores with strong absorbance near these wavelengths. Two-photon laser scanning fluorescence microscopy systems, on the other hand, are generally configured with a Ti:sapphire laser with 80–120 fs pulse output in the near-IR region (700–900 nm). Consequently, many typical single-photon fluorophores undergo only weak TPA in this region, since a fluorophore with λ_{max} of 490 nm would be expected to undergo two-photon absorption at ca 980 nm (a wavelength where the output power of commercial Ti:sapphire lasers is practically too low to be useful). Thus, commercial fluorophores are far from being optimized for use in two-photon fluorescence microscopy. A more reasonable absorption maximum for such chromophores is 380–420 nm (facilitating the use of near-IR femtosecond sources in the range 760–840 nm), since the TPA λ_{max} will be approximately twice the wavelength of the single-photon λ_{max}.[8]

RESULTS AND DISCUSSION

Two-photon absorbing compounds

Recent developments in the design of organic materials with large multiphoton absorptivity are based largely on the Type 2 TPA process outlined in Fig. 1, involving molecules that undergo large changes in dipole moment upon excitation from the ground to an excited state. A relatively limited number of two-photon absorbing compounds based on this premise have been reported. Among efficient TPA polar organic compounds are those with polarizable π-conjugated systems such as those reported with phenylethenyl,[10] fluorenyl[8,11–13] or polyenyl (bacteriorhodopsin and its analogs)[1] constructs bearing electron-donating (D) and/or electron-withdrawing (A) moieties, separated by a conjugated π-electron system, i.e., A–π–A, D–π–A, D–π–D. Femtosecond two-photon absorptivities for some of these materials are in the range 10–1000 GM.

As part of a program to establish an empirical body of non-linear absorptivity as a function of molecular structure, and to prepare efficient two-photon absorbing fluorophores, we have been investigating a series of compounds with systematic variation in molecular structure (Fig. 2).[8,11,12] Polar organic compounds such as 4-nitroaniline and 4-amino-4′-nitrobiphenyl undergo increases in dipole moments on photoexcitation from 6 to 14 D and from 6 to 20 D, respectively.[14] Thus, such compounds are expected to possess high two-photon absorptivity, as discussed above. We chose the fluorenyl ring system to serve as a thermally and photochemically stable π-conjugated analog of the 4,4′-disubstituted biphenyl derivatives. Locking the biphenyl unit into the fluorenyl ring provides greater electron delocalization

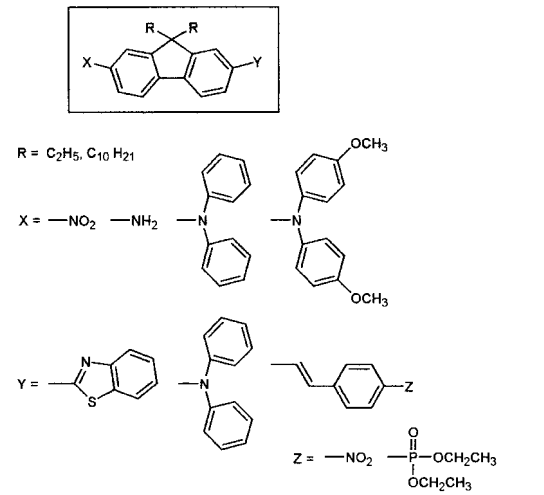

Fluorene Derivative	R	X	Y
1	C_2H_5	NPh_2	Z = 4-phosphonostyryl
2	C_2H_5	NPh_2	Z = 4-nitrostyryl
3	$C_{10}H_{21}$	NO_2	2-benzothiazolyl
4	$C_{10}H_{21}$	NH_2	2-benzothiazolyl
5	$C_{10}H_{21}$	NPh_2	2-benzothiazolyl
6	$C_{10}H_{21}$	$N(C_6H_4$-p-$OCH_3)_2$	2-benzothiazolyl
7	$C_{10}H_{21}$	NO_2	NPh_2
8	$C_{10}H_{21}$	NPh_2	NPh_2

Figure 2. Structures of selected fluorene derivatives that undergo TPA and up-converted fluorescence

through increased π molecular orbital overlap between the rings, enhancing molecular polarizability. Importantly, fluorene can be readily functionalized in the 2-, 7- and/or 9-positions. In addition to TPA optimization, another important molecular design aspect is wavelength sensitivity. Since commercially available Ti:sapphire lasers (output from 700 to 980 nm) are currently the most suitable light sources to provide the requisite high intensities for TPA, this must be considered in the design of TPA materials.

In order to prepare a series of derivatives for non-linear absorption studies, we sought the efficient preparation of key intermediates using synthetic methodology that would be readily adaptable for rapid functionalization. Ullmann condensation reactions of arylamines with aryl iodides and efficient Pd-catalyzed Heck and Stille coupling were employed to prepare a series of fluorene derivatives of varying electronic characteristics (Fig. 2).[8,11,12,15] The UV–visible absorption spectrum of phosphorylated fluorene derivative **1** in CH_3CN extended out to about 480 nm with two λ_{max}, one at 308 nm and the other at 383 nm. The visible absorption of nitro-containing fluorene derivative **2** in CH_3CN extended out to about 550 nm with two λ_{max}, one at 309 nm and the other at 414 nm. The fluorescence emission spectrum of **5** ranges from 400 to 630 nm with an emission λ_{max} of 475 nm upon excitation at 380 nm. Fluorene derivative **5** possesses highly desirable characteristics for use in

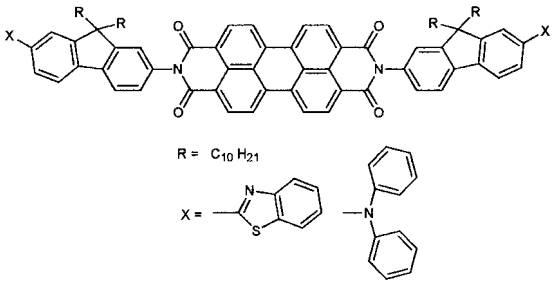

Perylene Derivative	X
8	2-benzothiazolyl
9	NPh_2

Figure 3. Structures of multifunctional TPA dyes with an electron-accepting perylene core

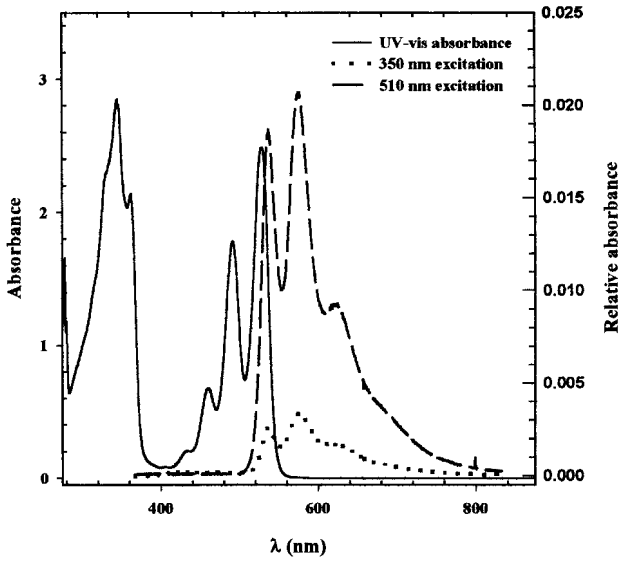

Figure 4. Overlay of UV–visible absorption spectrum (solid line) and fluorescence emission spectra of perylenediimide **8** in THF excited at 350 nm (dotted line) and 510 nm (dashed line)

two-photon fluorescence microscopy, since it has an absorption λ_{max} of 392 nm. The fluorescence emission spectrum of **6** ranged from 410 to 675 nm with an emission λ_{max} of 516 nm upon excitation at 400 nm. Fluorene derivative **6** also possesses highly desirable characteristics for use in two-photon fluorescence microscopy, i.e. it has an absorption λ_{max} of 408 nm.

Two-photon absorption measurements have been performed on several of these compounds using an NLO spectrometer and pump–probe experiment. Details of the experimental technique have been described elsewhere.[11] Briefly, non-degenerate TPA was measured using a pump–probe experiment in which TPA was induced by spatial and temporal overlap of a 1210 nm femtosecond pump beam and a femtosecond white light continuum (WLC) probe beam. The wavelength of the pump beam was selected as 1210 nm (the photon energy at this wavelength is not energetic enough to cause degenerate TPA). The probe beam consisted of a femtosecond white light continuum (WLC) generated by irradiation of a sapphire window in front of the sample.

Preliminary data indicate that the fluorene derivatives in Fig. 2 have high two-photon absorptivity. For example, at a WLC probe wavelength of 615 nm, diphenylaminobenzothiazolylfluorene (**5**) exhibited nondegenerate TPA of ca 820×10^{-50} cm^4 s photon^{-1} molecule^{-1} (820 GM). Fluorene **1** exhibited a maximum two-photon absorptivity of ca 650×10^{-50} cm^4 s photon^{-1} molecule^{-1} (650 GM) at WLC wavelength 605 nm, whereas the two-photon absorptivity of fluorene **2** was significantly higher, ca 1300×10^{-50} cm^4 s photon^{-1} molecule^{-1} (1300 GM) at WLC wavelength 670 nm. Evident from this comparison is an increase in TPA with a more polar molecular structure, indicative of a larger $\Delta\mu$ for **2** relative to **1**, and consistent with δ values expected for molecules that undergo large dipole moment changes upon photoexcitation. The large two-photon absorptivities and associated λ_{max} for the fluorene derivatives open the door for potential applications of these chromophores in multiphoton fluorescence imaging and other optical applications (as discussed below).

Next-generation multifunctional TPA materials are envisioned which incorporate functionality for high two-photon absorptivity along with molecular constructs for energy transfer, electron transport and/or morphological variation (Fig. 3). Driving our studies are potential applications of perylenediimide derivatives in molecular electronics applications such as organic photorefractive media for optical signal processing, electron-transporting components in organic light-emitting diodes, materials for electrophotography, n-type photovoltaic materials for solar energy conversion, fluorescent dyes and near-IR dyes.[15] We recently reported the synthesis of perylenediimide **8**.[15] Interestingly, perylenediimide **8** exhibited two strong UV–visible absorption bands (Fig. 4), one in the UV from 270 to 385 nm (λ_{max} = 345 nm) and another in the visible from 410 to 545 nm with λ_{max} at 457, 486 and 522 nm. The first absorption band is due to the fluorenyl groups, as it is similar to the absorption range exhibited by the aminofluorene **4** from 210 to 450 nm with λ_{max} = 380 nm, while the absorption in the visible range is due to the central perylene ring system.

The fluorescence emission spectrum of perylene **8** was obtained and is shown in Fig. 4, where excitation was performed at λ_{ex} = 325 nm, resulting in an unexpected emission λ_{max} at 540, 585 and 625 nm. Excitation at λ_{ex} = 510 nm resulted in a similar emission λ_{max} profile to that obtained with the λ_{ex} = 325 nm.[15]

The resulting emission profile from the first excitation (350 nm) is indicative of an intramolecular energy transfer process whereby the excited fluorenyl group undergoes energy transfer to the perylene ring system,

facilitating excitation followed by emission.[15] This then generates a similar emission spectrum to that obtained from $\lambda_{ex} = 510$ nm, although the relative intensity of the fluorescence from this energy transfer process is weaker than that of the corresponding fluorescence obtained from the excitation performed at the visible maxima owing, presumably, to competing deactivation processes. Since the longer wavelength absorption band at the perylene moiety overlaps with its emission, reabsorption of the emission in the range 500–560 nm is likely. The bisdiphenylaminoperylene derivative **9** (Fig. 3) exhibited similar luminescence behavior to the benzothiazole analog but striking differences in morphology were observed. Whereas the benzothiazole analog **8** was an amorphous glass with $T_g = 111\,°C$, the diphenylamino derivative **9** afforded large single crystals. DSC analysis of **9** revealed two melting endotherms at 160 and 297 °C, with corresponding cooling exotherms at 128 and 242 °C, respectively, demonstrating a degree of morphological control. We are currently investigating the basis of the morphology differences for these two derivatives through computational modeling.

Two-photon microfabrication

It is widely believed that a revolution in miniaturization, particularly in the field of microelectromechanical systems (MEMS), is under way. Figures predict the world's MEMS market to be more than $14 billion.[16] It is projected that the design and manufacturing technology that will be developed for MEMS may rival, or even surpass, the far-reaching impact of ICs on society and the world's economy. At the forefront of techniques being explored for 3-D spatially resolved materials imaging and processing are methods based on TPA. In contrast to the linear dependence of single-photon absorption on incident light intensity in conventional photopolymerization, the quadratic dependence of photoexcitation on light intensity in TPA can be exploited to confine polymerization to the focal volume and achieve fabrication of microstructures via 3-D spatially resolved polymerization.[5]

Two-photon absorption can occur in certain materials at wavelengths well beyond that which monomers, polymers and most organic substances absorb (one-photon), affording a greater depth of penetration, creating little or no damage to the host. Hence two-photon microfabrication via photoinitiated polymerization represents a potentially versatile technology that should be compatible with construction of mechanical, chemical, electrical, optical or biosensor systems. Additionally, it should be integratable with conventional IC processing technologies and femtosecond laser micromachining.

Although several reports of two-or multiphoton induced polymerization appeared in the literature as early as 1971,[17] most of these involve two or more sequential, resonant single-photon excitation processes at single or multiple wavelengths (i.e. excited state absorption).[18–20] The resonant processes must be distinguished from the simultaneous two-photon excitation process of concern here owing to the fundamental differences in achieving spatially resolved polymerization, i.e. a much higher degree of inherent 3-D spatial resolution in the simultaneous process. Less relevant to the current objectives are a limited number of accounts of two-photon induced polymerization in the gas phase.[21–24]

Two-photon photopolymerization of commercial acrylate monomer systems, preformulated with UV photoinitiators, has been reported, although little information regarding photoinitiators was available.[25–28] Two-photon absorbing compounds based on phenylethenyl constructs bearing electron-donating and/or electron-withdrawing moieties have been reported.[10] Among these are electron-rich derivatives that have been found to undergo a presumed two-photon induced electron transfer to acrylate monomers[29] or proposed fluorescence energy transfer to a photoinitiator,[30] initiating polymerization. The reportedly efficient two-photon photoinitiators, although more photosensitive than previously studied UV photoinitiators, are not commercially available and require involved syntheses. Hence the practicality of their broader use is questionable.

Recently, we reported the near-IR two-photon induced polymerization of (meth)acrylate monomers using a commercially available photoinitiator system based on a visible light-absorbing dye.[5] Two-photon initiated polymerization was conducted at 775 nm via direct excitation of a commercially available dye (5,7-diiodo-3-butoxy-6-fluorone, H-Nu 470) in the presence of an arylamine, and (meth)acrylate monomer. The fluorone dye, 5,7-diiodo-3-butoxy-6-fluorone (H-NU 470), and *N*,*N*-dimethyl-2,6-diisopropylaniline were obtained from Spectra Group; thick films were cast on glass slides from neat mixtures and thin films were obtained via spin coating from a dioxane solution, resulting in an electron-transfer free radical initiation process. The excitation wavelength was well beyond the linear absorption spectrum for 5,7-diiodo-3-butoxy-6-fluorone (strong and weak absorption maxima at 330 and 470 nm, respectively). Four commercial acrylate and methacrylate monomer systems were used: ethoxylated bisphenol A diacrylate (SR349, Sartomer), pentaacrylate ester (SR9041, Sartomer), aromatic urethane acrylate blended with tripropylene glycol diacrylate (CN973A80, Sartomer), and 2-methyl-2-propenoic acid (1-methyethylidene)-bis(4,1-phenyleneoxy-2-hydroxy-1,3-propanediyl) ester (BisGMAx950, Esschem).

According to the mechanism deduced from single-photon photochemical studies of the initiating system (Fig. 5),[31] electron transfer from the aromatic amine (*N*,*N*-dimethyl-2,6-diisopropylaniline, DIDMA) to the fluorone derivative, followed by proton transfer from the amine to the fluorone, resulted in formation of an

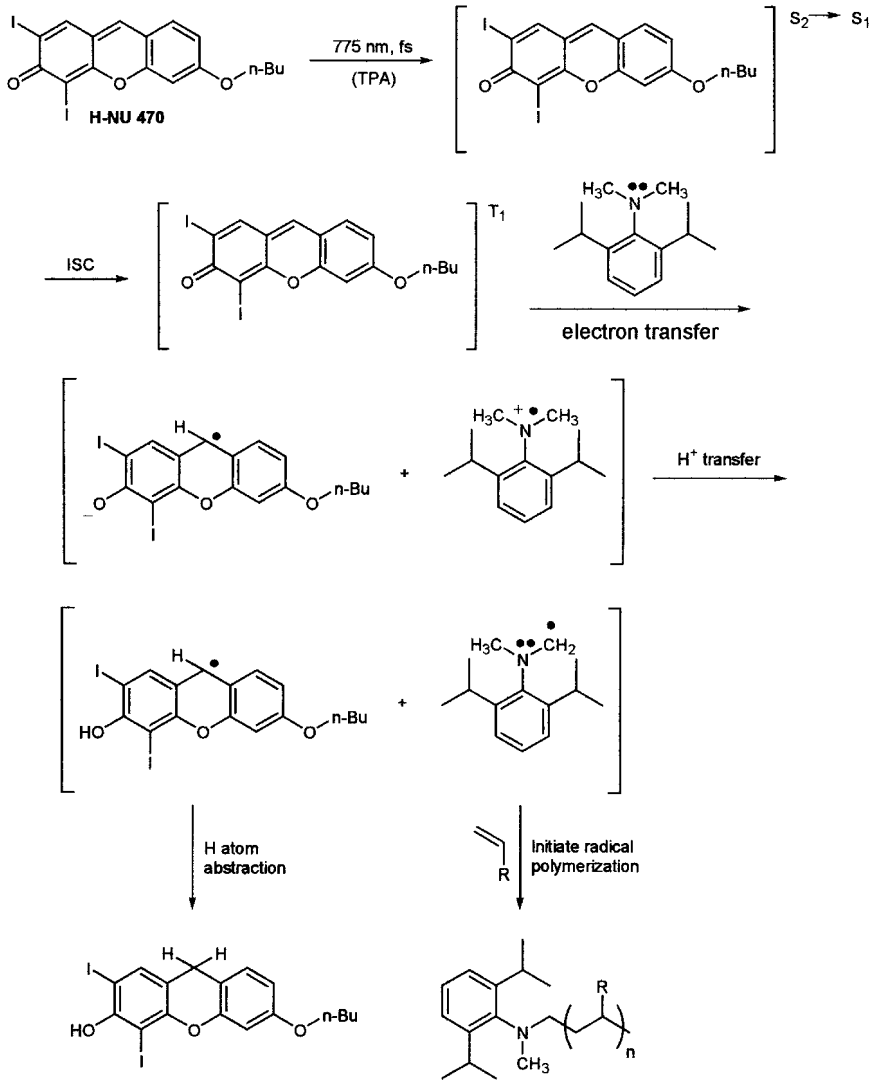

Figure 5. Direct two-photon photoinitiated polymerization at 775 nm

arylamine bearing a free radical localized on the α-methylene carbon. This free radical species then initiated polymerization of (meth)acrylate derivatives. A diaryliodonium salt can be added to accelerate the rate of polymerization.

A number of control experiments were performed to support a two-photon based excitation process. First, experiments were performed using a Ti:sapphire laser in continuous wave (CW) vs mode-locked (80 fs pulse width). Polymerization was not observed in CW mode, while polymerization occurred only when the laser was mode-locked. Next, experiments were performed on monomer alone (no initiator), in which no polymerization was observed upon exposure to near-IR femtosecond radiation. Furthermore, an initiator system comprised of isopropylthioxanthone (ITX) and DIDMA (monomer:-ITX:DIDMA mole ratio $1{:}1.4 \times 10^{-3}{:}5.4 \times 10^{-3}$) also afforded polymer in the presence of an acrylate monomer under near-IR femtosecond irradiation, attesting to the generality of the electron transfer polymerization discussed above. Similarly, no polymer was produced when the ITX–DIDMA–acrylate mixture was exposed to the same wavelength in CW mode.

The formation of polymeric microstructures with a variety of dimensions was accomplished with the H-NU 470 initiator–acrylate monomer system [Fig. 7(a)]. Similar 2-D microstructures were obtained via two-

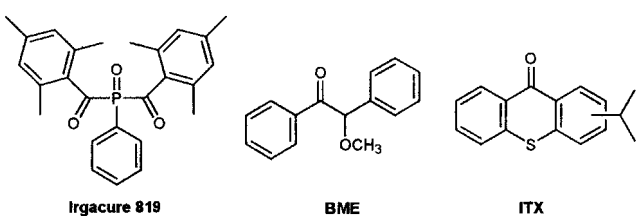

Figure 6. Free-radical photoinitiators for near-IR two-photon polymerization

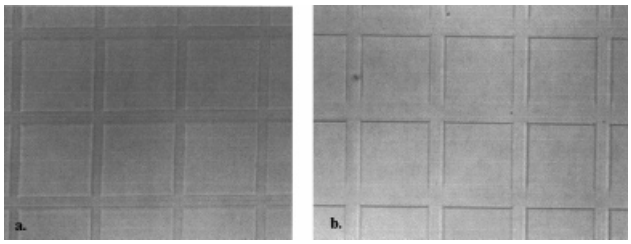

Figure 7. Optical micrographs of grid-type microstructures created via two-photon polymerization of an acrylate monomer (SR349) (a) using the H-NU 470 initiating system (9 μm linewidth, 100 μm line spacing) and (b) using fluorene **5** as initiator (18 μm linewidth, ~100 μm line spacing)

photon polymerization of acrylate monomers using commercial photoinitators and a 775 nm femtosecond laser. In particular, ary ketone photoinitiators (Fig. 6) such as isopropylthioxanthone (ITX), benzoin methyl ether (BME) and an acylphosphine oxide (Irgacure 819, CIBA) were found to be effective initiators (all have λ_{max} <400 nm), resulting in well-defined microstructures. Typical monomer:initiator molar ratios were $1{:}3.5 \times 10^{-4}$ (ITX), $1{:}7.5 \times 10^{-3}$ (BME), $1{:}1.1 \times 10^{-3}$ (Irgacure 819) and $1{:}1.9 \times 10^{-3}$ (fluorene **5**, Fig. 2). In addition, compositions comprised of acrylate monomer SR349, ITX and *N*-ethyldiethanolamine, or SR349, H-NU 470 and *N*-ethyldiethanolamine in $1{:}3.2 \times 10^{-3}{:}0.36$ or $1{:}7.2 \times 10^{-4}{:}0.32$ molar ratios, respectively, were effective in forming microstructures upon two-photon excitation (TPE).

The strong two-photon absorbing compound fluorene **5** was an effective initiator for an acrylate polymerization via TPE at 775 nm, presumably by means of an electron-transfer process. The resulting microstructure using fluorene **5** and SR349 acrylate had 18 μm linewidths of uniform spacing [Fig. 7(b)]. In a simple grid scan, linewidths of 9 μm, spaced 100 μm apart, were produced with the H-NU 470 system. Microstructures were readily examined by optical reflection microscopy.

A logical frontier is the preparation of functional microstructures. The fabrication of magnetically actuated microstructures via two-photon polymerization is envisioned. This was demonstrated via two-photon free radical polymerization of an acrylate monomer (SR349), with the H-NU 470–DIDMA initiator system, containing emulsion-stabilized magnetite nanoparticles. Optical microscope and AFM imaging revealed the microstructure and the presence of the magnetite nanoparticles entrapped in the polymeric microstructure (Fig. 8). In a polymerized grid-type microstructure containing magnetite nanoparticles, the optical micrograph revealed a structure with 18 μm horizontal linewidth. AFM topographic imaging of a small section of the microgrid was accomplished in broad band mode (50 kHz vibration), indicating a 300 nm average thickness of the polymer. AFM imaging in error mode (50 kHz vibration) showed a relatively even distribution of the nanometallic particles in the polymerized and unpolymerized areas.

Cationic photoinitiated polymerization of epoxides, vinyl ethers and methylenedioxolanes has received increasing attention, owing in large part to the oxygen insensitivity of the cationic process.[32] Commercially available diaryliodonium (CD-1012, Sartomer) and

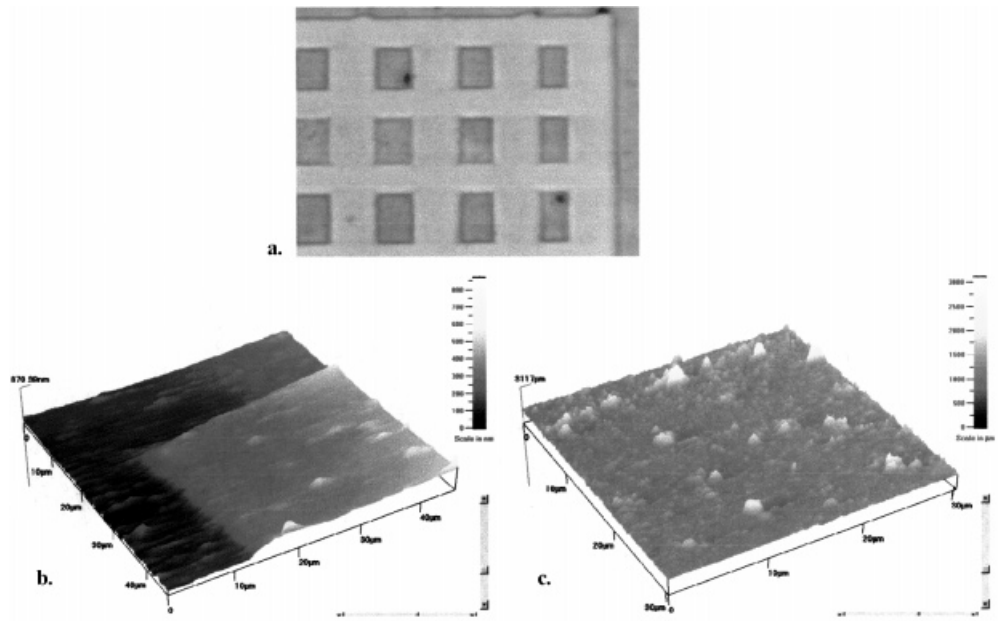

Figure 8. Polymerized grid-type microstructure containing magnetite nanoparticles: (a) optical micrograph (18 μm horizontal linewidth), (b) AFM topographic image of partial microgrid in broad band mode (50 kHz vibration) and (c) nanometallic particles in error mode (50 kHz vibration)

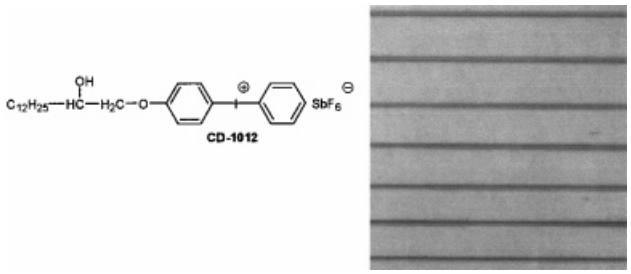

Figure 9. Optical microscopy image (right) of microstructures (18 μm linewidth, progressively increasing line spacing beginning with 72 μm, from bottom to top) formed via the two-photon cationic polymerization of a mixture of poly(bisphenol A-*co*-epichlorohydrin) glycidyl end-capped and 3,4-epoxycyclohexylmethyl 3,4-epoxycyclohexanecarboxylate (K126, Sartomer) using CD-1012 (left)

triarylsulfonium (CD-1010, Sartomer) salts were found to initiate polymerization of multifunctional epoxide and vinyl ether monomers, affording well-defined microstructures (Figs 9 and 10). Typical multifunctional epoxide monomers investigated were a mixture of poly(bisphenol A-*co*-epichlorohydrin, glycidyl end-capped and 3,4-epoxycyclohexylmethyl 3,4-epoxycyclohexanecarboxylate (K126, Sartomer) or Epon SU-8 (Shell) and K126 in 1:4 weight ratios, respectively, with 1 wt% of either the sulfonium or iodonium initiators. In Fig. 9, the linewidth is 18 μm with progressively increasing line spacing, from bottom to top, beginning at 72 μm (as programmed with the computer-controlled scanner). The microstructure in Fig. 10 has 18 μm linewidths with 72 μm line spacing. The versatility of two-photon polymerization is now well positioned to allow the fabrication of complex three-dimensional microstructures, a prospect we are currently pursuing.

Two-photon photochemical transformations for advanced optical applications

Over the past 50 years, the field of organic photochemistry has produced a wealth of information, from reaction mechanisms to useful methodology for synthetic transformations. Many technological innovations have been

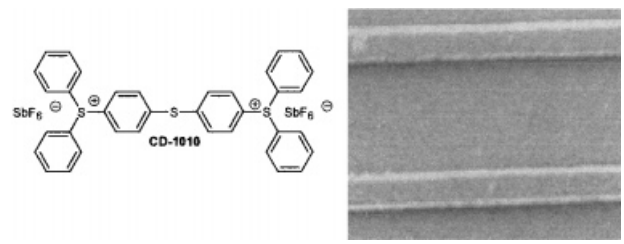

Figure 10. SEM image (right, 250 × magnification) of microstructure (18 μm linewidth, 72 μm line spacing) formed via the two-photon cationic polymerization of Epon SU-8 (Shell) and K126 with CD-1010 (left)

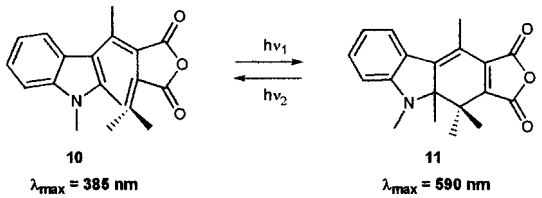

Figure 11. Photoisomerization of fulgide **10**

realized during this time due to the exploits of this knowledge, including photoresists and lithography for the production of integrated circuits, photodynamic therapy for cancer treatment, photoinitiated polymerization, UV protection of plastics and humans through the development of UV absorbing compounds and sunscreens, and fluorescence imaging, to name a few. These processes involve 'single-photon' absorption-based photochemistry. Comparatively few studies of multiphoton-induced organic photochemistry have been reported.

In most books on organic photochemistry there is scarcely a mention of simultaneous two-photon induced photochemistry, e.g. in *Electronic Aspects of Organic Photochemistry*, the only mention of this was 'Simultaneous absorption of two photons is also possible and occurs when very high light intensities are used,'[33] while just brief descriptions can be found in *Excited States in Organic Chemistry*[34] and *Principles and Applications of Photochemistry*.[35] This said, the underlying principles of multi- or two-photon absorption are particularly meritorious, and warrant much further investigation (particularly with the advent of commercially available ultrafast pulsed lasers). In fact, the field of two-photon organic photochemistry is in its infancy, not unlike the field of single-photon organic photochemistry 50 years ago.

Rentzepis and co-workers reported two-photon induced photochromism of spiropyran derivatives at 1064 nm.[36,37] Analogous to single-photon absorption facilitated isomerization, the spiropyran underwent ring-opening isomerization to the zwitterionic colored merocyanine isomer. The merocyanine isomer underwent TPA at 1064 nm, resulting in up-converted fluorescence. Spiropyrans are known to undergo photobleaching and photodegradation upon prolonged exposure, and hence are not suitable for long term use. Nonetheless, an intriguing model for 3-D optical storage memory was proposed.

Like many spiropyrans, spirooxazine and fulgide-type compounds are known to undergo photoisomerization from a colorless to highly colored isomer.[38] Unlike the spiropyrans, the thermally and photochemically stable spirooxazine and fulgide-type compounds have been reported which underwent numerous single-photon photochemical isomerization (color) and reversion cycles without significant degradation.[39] Optical data recording potentials as high as 10^8 bits cm^{-2} have been reported for fulgide-type materials. In an effort to develop a more photostable material for two-photon holographic imaging

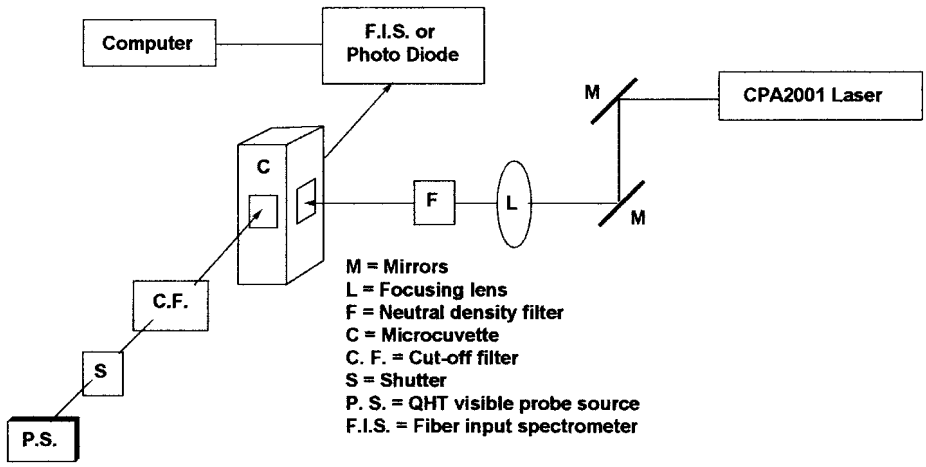

Figure 12. Optical system for pump–probe photoisomerization kinetics experiment

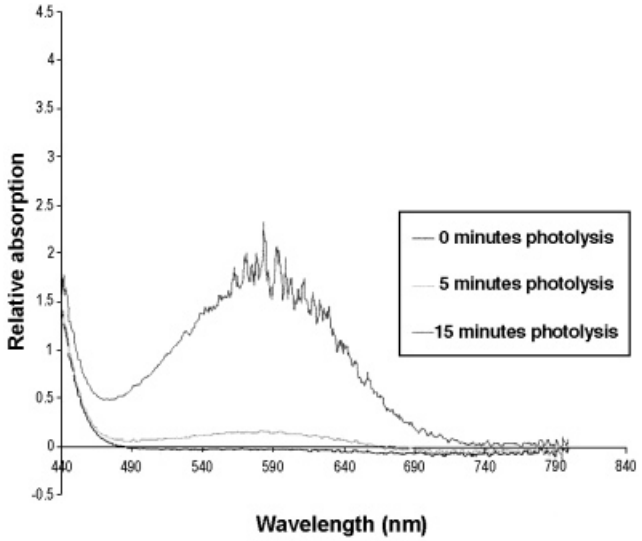

Figure 13. Absorption spectra as a function of time for the two-photon induced photoisomerization of fulgide **10**

and information storage, flugide **10** (λ_{max} = 385 nm) was chosen for study, particularly since its single-photon photochromic behavior is well established (Fig. 11).[40]

First, to demonstrate the possibility of two-photon induced photochromism for **10**, determination of the kinetics of femtosecond near-IR (775 nm) photoisomerization was performed using a pump–probe experimental setup (Fig. 12) to verify the two-photon induced nature of the transformation.

As seen in Fig. 13, formation of the fulgide photoisomer **11** was monitored as a function of time. Plots of absorbance at 585 nm (log I_0/I) versus time (s) were linear for the formation of the ring-closed photoisomer. The photoisomerization rate constants thus obtained were $2.53 \times 10^{-3} \pm 0.3 \times 10^{-3}$ and $6.99 \times 10^{-3} \pm 0.5 \times 10^{-3} s^{-1}$ at irradiation intensities of 3.5 and 7.0 mW, respectively. As can be seen from the rate constants as a function of irradiant intensity, a near-quadratic dependence was observed for the photoisomerization of **10** as a function of intensity of the 775 nm femtosecond pump beam, supportive of a two-photon induced process.

Next, preliminary 2-D interferometric recording was performed using a Mach–Zehnder interferometry setup using a Clark CPA2001 775 nm femtosecond laser as the irradiation source (Fig. 14). Photoinduced changes were observed in the regions of high light intensity (bright interference fringes) in a thin film of poly (styrene)–fulgide **10** composite, demonstrating a proof of principle for effecting photochromic transformations

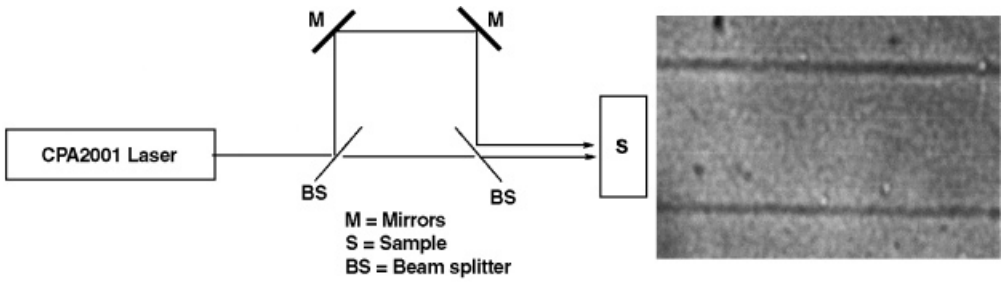

Figure 14. Schematic diagram of a Mach–Zehnder interferometer for 2-D recording via two-photon photochromism (left). Dark lines in right image result from high-intensity bright fringe-induced photoisomerization of fulgide **10** in a polystyrene film (13 μm linewidth and 155 μm line spacing)

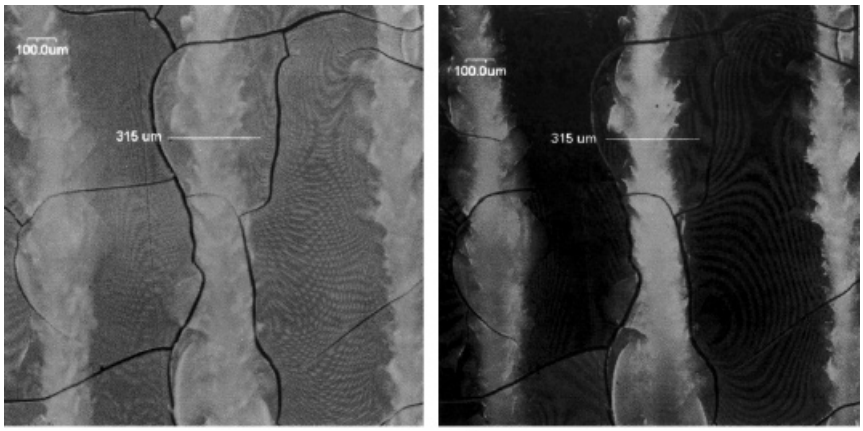

Figure 15. Comparative *xy* (lateral) images of fluorene **6**-doped PMMA on scored glass slide via (a) single-photon excitation (Ar, 488 nm) LSCM and (b) two-photon (Ti:sapphire, 815 nm) LSM. Both images were taken from the same focal plane

in localized regions (Fig. 14) as a model for holographic information storage. The dark lines in the image of Fig. 14 result from high intensity bright fringe-induced photoisomerization of fulgide **10** (13 μm linewidth and 155 μm line spacing). Current efforts involve two-photon holographic volumetric recording in this material.

Non-destructive 3-D multiphoton fluorescence imaging

The use of longer wavelength light as the excitation source for fluorescence emission leads to deeper penetration depths than possible with conventional UV or visible fluorescence techniques. Since the fluorescence emission is confined to the focal volume in the two-photon process, there will be virtually no out of focus fluorescence signal, i.e. two-photon excitation falls off rapidly away from the focal volume, resulting in a high signal-to-noise ratio. An advantage of excitation with near-IR radiation is that most materials are transparent in this region. In practice, one is able to image twice as deep in samples using two-photon induced fluorescence compared with conventional confocal single-photon fluorescence microscopy.[9]

For example, use of two-photon fluorescence imaging in the biological sciences ranges from the study of the dynamics of the cytoskeleton in the nematode *C. elegans*,[41] studies of the mechanism by which myoblasts take up DNA,[42] studies of the distribution of mitochondria in developing mammalian embryos,[43] neural transplant processes,[44] 3-D time-lapse imaging of living neurons,[45] lipid membrane dynamics,[46] dendritic spines and other neuronal microdomains,[47] microtubule dynamics in living cells,[48] to the photoactivated release of caged compounds[49] and NADH photoactivation.[50]

Two-photon laser scanning microscopy is a potentially useful, non-destructive tool to study surfaces, interfaces and fractures in polymer or glass specimens. Non-destructive evaluation refers to a non-invasive technique for probing interior microstructure and subsurface features. Recently, fractures in polymer samples were reportedly imaged by this technique.[51] Two-photon multichannel fluorescence microscopy was also demonstrated to be useful to probe and construct images of multilayered coatings. Figure 15 provides a direct comparision of non-destructive, normal laser scanning confocal microscopic (LSCM) (single-photon) imaging vs two-photon laser scanning microscopic (LSM) imaging of a fluorophore-labeled polymer. Fluorene **6** (Fig. 2) and poly(methyl methacrylate) (PMMA) were dissolved in THF and cast on a scored (scratched) glass substrate.

Comparative lateral (*xy*) images (512 × 512 pixel size, 10 × objective, numerical aperture 0.3) were obtained, whereby both the single-photon (SPE) and two-photon (TPE) excitation of the fluorophore-doped polymer on the glass surface were scanned from the same focal plane within the substrate. SPE was accomplished with a CW argon ion laser (488 nm), and the fluorescence emission was detected by a photomultiplier tube after passage through a 60 μm confocal aperture to reduce out-of-focus fluorescence. Clearly evident in the TPE upconverted fluorescence image (Fig. 15) is the higher contrast resulting from virtually no out-of-focus fluorescence, an inherent manifestation of the TPA process. In two-photon imaging, no confocal aperture was used.

Owing to the quadratic dependence of the TPA process on incident intensity, resulting in minimal out-of-focus emission, a large improvement in emission signal-to-noise ratio is expected. This is borne out in Fig. 16 in which the emission intensity is plotted versus position across the fluorophore-doped polymer in one of the scores [315 μm lines in Fig. 15(a) and (b)]. In addition to an enormous increase in the signal-to-noise ratio, a large

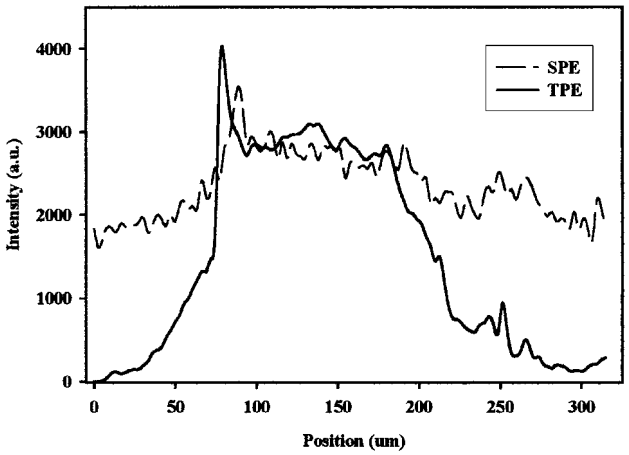

Figure 16. Plots of SPE and TPE emission intensity across the fluorophore-doped polymer in one of the scores [315 μm lines in Fig. 15(a) and (b)]

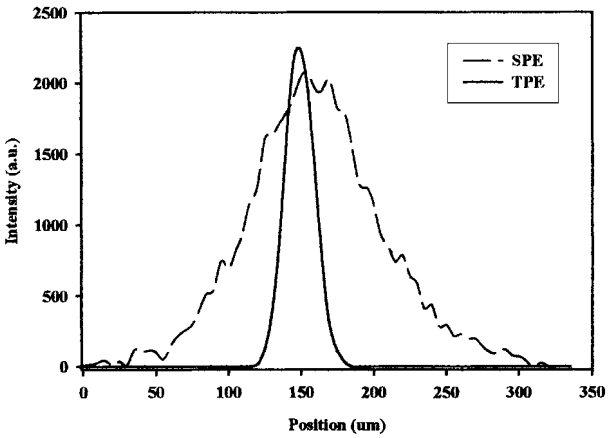

Figure 18. Plots of SPE and TPE emission intensity across cross-sectioned (*xz*) images of the fluorophore-doped polymer in one of the scores [335 μm lines in Fig. 17(a) and (b)]

increase in the sensitivity is also observed, as no confocal aperture is used to block emission from the two-photon image.

Both single- and two-photon laser scanning microscopic sectioning can be employed to collect non-destructive cross-sectional images of polymer films. Figure 17(a) and (b) show fluorescence emission across an *xy* line as a function of depth (5 μm *z* steps over 340 μm). Figure 17(a) displays the cross-sectional image of the same polymer-coated scored substrate, as shown in Fig. 15, obtained via single-photon laser scanning confocal microscopy (488 nm excitation). In contrast, Fig. 17(b) is the same cross-sectional area imaged via two-photon excitation. Obvious in these images is the substantial increase in resolution, i.e. the single-photon laser scanning confocal microscopic image exhibits out-of-focus fluorescence. The two-photon image is clearly much better defined, providing information on the interfacial micromorphology between the coating and the substrate.

A plot of emission intensity versus depth through the film thickness [along the 335 μm yellow line in Fig. 17(a) and (b)] allows direct comparison of resolution for single- versus two-photon fluorescence imaging (Fig. 18). A remarkable difference is observed with a better resolved signal obtained via TPE, corresponding approximately to the film thickness.

The advantages of two-photon fluorescence imaging of polymer films and interfaces, relative to conventional LSCM, are clear. One can anticipate the widespread application of this technique as a non-destructive tool for materials and interfacial micromorphological imaging in the future.

Photodynamic therapy (PDT)

Two-photon activation of photodynamic cancer therapeutic agents should be advantageous since most tissue is transparent to near-IR radiation, affording much deeper penetration depths (allowing subcutaneous treatment). Importantly, the spatial resolution inherent in 2PA will provide increased resolution (localization) in photoactivation of the agent. Psoralen derivatives have been investigated for near-IR femtosecond excitation and have been found to crosslink DNA via $\pi 2s + \pi 2s$ photocycloaddition between psoralen C=Cs and pyrimidine bases of DNA.[52] This results in cell death through inhibiting DNA replication. In addition, porphyrin derivatives have been shown to be effective singlet oxygen sensitizers upon irradiation *in vivo* (via both single- and two-photon excitation), resulting in tumor cell death.[53] In fact, a porphyrin derivative (Photofrin), approved by the FDA for the treatment of a limited number of cancer types, is gaining increased acceptance in the USA. As PDT becomes a primary therapeutic practice, the advantages associated with highly localized TPA will allow better control of site-specific drug photoactivation.

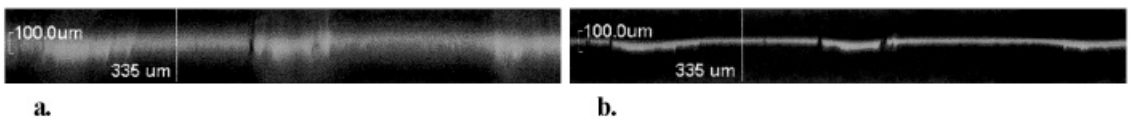

Figure 17. Cross-sectional (*xz*) image of the polymer coated glass substrate: (a) single-photon LSCM and (b) two-photon LSM images

In conclusion, the many advantages associated with non-linear absorption-induced processes is fast propelling two-photon absorbing materials to the forefront of several important fields. As the design criteria for increasing multiphoton absorptivity continue to evolve, more efficient TPA organic materials will be sought and prepared. Such materials can be used in 3-D volumetric optical recording, non-destructive 3-D imaging, optical sensor protection, photodynamic therapy and 3-D microfabrication. We can expect to witness breakthroughs in years to come, due to the harnessing of multiphoton absorption in organic materials.

EXPERIMENTAL

Femtosecond optical system for microfabrication and photoisomerization experiments. A laser system (CPA-2001 from Clark-MXR with an Er-doped fiber ring oscillator seeding a Ti:sapphire regeneration amplifier) was used to generate 775 nm light with a 150 fs pulse width at a repetition rate of 1 kHz and ~3 mW average power (~15 μJ per pulse).[14] The beam width was approximately 10 μm. A computer-controlled motorized *xy* step scanner was employed with a scan rate of 1 mm s^{-1}. Monomer/initiator films were spin-coated on glass slides and exposed to the near-IR laser using a variety of scan patterns. Exposed films were imaged using an optical light microscope in reflection mode or by SEM.

Laser scanning microscopy system. The laser scanning microscopy system consisted of an Olympus IX70 inverted microscope and Fluoview confocal laser scanning system fitted with a CW argon ion laser (488 nm, 5 mW) and mode-locked Ti:sapphire laser (80 MHz repetition rate, 120 fs pulse width, 815 nm, 50 mW) pumped with a 5 W frequency-doubled Nd:YAG diode laser (Spectra-Physics Millenia, 532 nm).

Materials. The synthesis and characterization of fluorene derivatives **1–7** are reported in Refs. 8 and 12. The synthesis and characterization of perylenediimide derivatives **8** and **9** are reported in Ref. 15. 2,9-Bis(9,9-didecyl-7-diphenylaminofluoren-2-yl)perylenediimide (**9**): UV–visible (THF): λ_{max} = 261, 309 and 355 nm (235–415 nm) and λ_{max} = 455, 488 and 523 nm (415–586 nm). Elemental analysis for $C_{114}H_{124}N_4O_4$: calculates C, 84.82 H, 7.74, N 3.47%; found C, 84.84 H, 7.88 N, 3.33% ^{1}H NMR (200 MHz, $CDCl_3$): δ (ppm) 8.72, 8.70 (d, 4H, ArH), 8.59, 8.55 (d, 4H, ArH), 7.79, 7.75 (d, 2H, ArH), 7.63, 7.58 (d, 2H, ArH), 7.38, 7.36 (dd, 2H, ArH), 7.30, 7.29 (dd, 2H, ArH), 7.27 (dd, 8H, ArH), 7.23 (s, 2H, ArH), 7.16, 7.12 (bm, 4H, ArH), 7.02 (bm, 8H, ArH), 1.90 (bm, 8H, CH_2), 1.20 (bm, 28H, CH_2), 1.10 (bm, 28H, CH_2), 0.90–0.70 (bm, 20H, CH_2, CH_3). ^{13}C NMR (50 MHz, $CDCl_3$), tentative assignments based on calculated values: δ (ppm) 163.1 (peryl. C1), 152.5 (C10), 151.8 (C13), 147.9 (C2′), 147.3 (C2), 141.5 (C7), 135.5 (peryl. 18), 134.0 (C12), 132.9 (C11), 131.1 (peryl. 15), 129.1 (peryl. C19), 128.9 (C4′), 128.5 (peryl. C4), 127.5 (C4), 125.8 (C5), 123.8 (peryl. C16), 123.4 (C5′), 122.9 (C1), 122.5 (C3′), 120.8 (C8), 119.7 (C3), 119.2 (C6). FT-IR (KBr, cm^{-1}): 3060, 3033 (ArCH), 2923, 2851 (alCH), 1703, 1665 (C=O). Fulgide **10** was prepared according to a published procedure.[40] All other materials (monomers and photoinitiators) were obtained from commercial sources, as identified in the text.

Acknowledgements

The National Science Foundation (ECS-9970078, DMR9975773) and the Air Force Office of Scientific Research (F49620-93-C-0063) are acknowledged for partial support of this research. K.D.B. thanks the Research Corporation for a Cottrell College Science Award (CC5051) and the Petroleum Research Fund of the American Chemical Society (35115-B4) for partial support of this work. K.D.B. and K.J.S. gratefully acknowledge the Air Force Office of Scientific Research for a Summer Faculty Research Fellowship and Summer Graduate Student Research Fellowship at the Air Force Research Laboratory's Polymer Branch, Wright-Patterson AFB, respectively. The authors thank Professor Meigong Fan of the Institute of Photographic Chemistry, Chinese Academy of Sciences, for assistance in preparing the fulgide derivative.

REFERENCES

1. Birge RR, Parsons B, Song QW, Tallent JR. In *Molecular Electronics*, Jortner J, Ratner M (eds). Blackwell Science: London, 1997; Chapt. 15.
2. Bhawalkar JD, He GS, Prasad PN. *Rep. Prog. Phys.* 1996; **59**: 1041.
3. Herman B, Wang XF, Wodnicki P, Perisamy A, Mahajan N, Berry G, Gordon G. In *Applied Fluorescence in Chemistry, Biology, and Medicine*, Rettig W, Strehmel B, Schrader S, Seifert H (eds). Springer: New York, 1999; 496–500.
4. Wu ES, Strickler JH, Harrell WR, Webb WW. *Proc. SPIE* 1992; **1674**: 776.
5. Belfield KD, Ren X, Van Stryland EW, Hagan DJ, Dubikovski V, Meisak EJ. *J. Am Chem. Soc.* 2000; **122**: 1217.
6. Goeppert-Mayer, M. *Ann. Phys.* 1931; **9**: 273.
7. Kershaw S. In *Characterization Techniques and Tabulations for Organic Nonlinear Optical Materials*, Kuzyk MG, Dirk CW (eds). Marcel Dekker: New York, 1998; Chapt. 7.
8. Belfield KD, Schafer KJ, Mourad W. *J. Org. Chem.* 2000; **65**: 4475.
9. Denk W, Strickler JH, Webb WW. *Science* 1990; **248**: 73.
10. Albota M, Beljonne D, Bredas, J-L, Ehrlich JE, Fu J-Y, Heikal AA, Hess SE, Kogej T, Levin MD, Marder SR, McCord-Moughon D, Perry JW, Rockel H, Rumi M, Subramaniam G, Webb WW, Wu X-L, Xu C. *Science*, 1998; **281**: 1653.
11. Negres RA, Van Stryland EW, Hagan DJ, Belfield KD, Schafer KJ, Przhonska OV, Reinhardt BA. *Proc. SPIE* 1999; **3796**: 88.
12. Belfield KD, Hagan DJ, Van Stryland EW, Schafer KJ, Negres RA. *Org. Lett.* 1999; **1**: 1575.

13. Reinhardt BA, Brott LL, Clarson SJ, Dillard AG, Bhatt JC, Kannan R, Yuan L, He GS, Prasad PN. *Chem. Mater.* 1998; **10**: 1863.
14. Coyle JD. In *Introduction to Organic Photochemistry*. Wiley: New York, 1986; 16.
15. Belfield KD, Schafer KJ, Alexander MD Jr. *Chem. Mater.* 2000; **12**: 1184.
16. Microelectromechanical Systems. Report by the Committee on Advanced Materials and Fabrication Methods of Microelectromechanical Systems, National Materials Advisory Board, Commission of Engineering and Technical Systems, National Research Council, NMAB-483. National Academy Press: Washington, DC, 1997.
17. Chin SL, Bedard G. *Phys. Lett.* 1971; **36A**: 271.
18. Ichimura K, Sakuragi M. *J. Polym. Sci., Part C: Polym. Lett.* 1988; **26**: 185.
19. Jent F, Paul H, Fischer H. *Chem. Phys. Lett.* 1988; **146**: 315.
20. Lougnot DJ, Ritzenthaler D, Carre C, Foussier JP. *J. Appl. Phys.* 1988; **63**: 4841.
21. Papouskova Z, Pola J, Bastl Z, Tlaskal J. *J. Macromol. Sci. Chem.* 1990; **A27**: 1015.
22. Morita H, Sadakiyo T. *J. Photochem. Photobiol. A* 1995; **87**: 163.
23. Morita H, Semba K, Bastl Z, Pola J. *J. Photochem. Photobiol. A* 1998; **116**: 91.
24. El-Shall MS, Daly GM, Yu Z, Meot-Ner M. *J. Am. Chem. Soc.* 1995; **117**: 7744.
25. Strickler JH, Webb WW. *Opt. Lett.* 1991; **16**: 1780.
26. Maruo S, Nakamura O, Kawata S. *Opt. Lett.* 1997; **22**: 132.
27. Borisov RA, Dorojkina GN, Koroteev NI, Kozenkov VM, Magnitskii SA, Malakhov DV, Tarasishin AV, Zheltikov AM. *Appl. Phys. B* 1998; **67**: 765.
28. Borisov RA, Dorojkina GN, Koroteev NI, Kozenkov VM, Magnitskii SA, Malakhov DV, Tarasishin AV, Zheltikov AM. *Laser Phys.* 1998; **8**: 1105.
29. Cumpston BH, Ananthavel SP, Barlow S, Dyer DL, Ehrlich JE, Erskine LL, Heikal AA, Kuebler SM, Lee IYS, McCord-Maughon D, Qin J, Rockel H, Rumi M, Wu XL, Marder SR, Perry JW. *Nature (London)* 1999; **398**: 51.
30. Joshi MP, Pudavar HE, Swiatkiewicz J, Prasad PN, Reinhardt BA. *Appl. Phys. Lett.* 1999; **74**: 170.
31. Hassoon S, Neckers DC. *J. Phys. Chem.* 1995; **99**: 9416.
32. Belfield KD, Abdelrazzaq FB. *J. Polym. Sci. Part A: Polym. Chem.* 1997; **35**: 2207;; Belfield KD, Abdelrazzaq FB. *Macromolecules* 1997; **30**: 6985.
33. Michl J, Bonacic-Koutecky V. *Electronic Aspects of Organic Photochemistry*. Wiley: New York, 1990; 63.
34. Barltrop JA, Coyle JD. *Excited States in Organic Chemistry*. Wiley: New York, 1975; 46.
35. Wayne RP. *Principles and Applications of Photochemistry*. Oxford University Press: New York, 1988; 58–63.
36. Parthenopoulos DA, Rentzepis PM. *Science* 1989; **245**: 843.
37. Dvornikov AS, Rentzepis PM. *Opt. Commun.* 1995; **119**: 341.
38. Durr H, Bouas-Laurent H (eds). *Photochromism Molecules and Systems*. Elsevier: New York, 1990; Chapt. 8–10.
39. Heller HG. In *CRC Handbook of Photochemistry and Photobiology*, Horspool WM, Song PS (eds). CRC Press: Boca Raton, FL, 1995; 181.
40. Janicki SZ, Schuster GB. *J. Am. Chem. Soc.* 1995; **117**: 8524.
41. Lavin CA, Mohler WA, Keating HH, White JG. *Microsc. Microanal.* 1997; **3**: 291.
42. Conklin M, Centonze V, Wolff M, Coronado R. *Biophys. J.* 1998; **74**: A355.
43. Wokosin DL, White JG. *Proc. SPIE* 1998; **3269**: 86.
44. Potter SM, Pine J, Fraser SE. *Scanning Microsc.* 1996; Suppl. 10: 189.
45. Potter SM, Fraser SE, Pine J. *Scanning* 1996; **18**: 147.
46. Parasassi T, Gratton E, Yu WM, Wilson P, Levi M. *Biophys. J.* 1997; **72**: 2413.
47. Yuste R, Denk W. *Nature (London)* 1995; **375**: 682.
48. Hird S, Frohlich V, White J. *Am. Soc. Cell Biol.* 1994; **34**: H144.
49. Caucheteux-Silberzan I, Williams RM, Webb WW. *Biophys. J.* 1993; **64**: A109.
50. Piston DW, Masters BR, Webb WW. *J. Microsc.* 1995; **178**: 20.
51. Bhawalkar JD, Shih A, Pan SJ, Liou WS, Swiatkiewicz J, Reinhardt BA, Prasad PN, Cheng PC. *Bioimaging* 1996; **4**: 168.
52. Fisher WG, Partridge WP Jr, Dees C, Wachter EA. *Photochem. Photobiol.* 1997; **66**: 141.
53. Ressler MM, Pandey RK. *CHEMTECH* 1998; **28**(3): 39.

